Nature Environment and Pollution Technology
An International Quarterly Scientific Journal

p-ISSN: 0972-6268
(Print copies up to 2016)
e-ISSN: 2395-3454

Vol. 19 | No. 4 | pp. 1465-1474 | 2020

Original Research Paper

https://doi.org/10.46488/NEPT.2020.v19i04.012

Open Access Journal

Ethylenediaminetetraacetic Dianhydride (EDTAD) Modified Coconut Frond for Removal of Pb(II) Ions: Kinetics, Isotherm and Thermodynamic

Nur Ain Mohd Nizam Prushotman*, Megat Ahmad Kamal Megat Hanafiah†, Noorul Farhana Md Ariff*** and Shariff Ibrahim*****

*Faculty of Applied Sciences, Universiti Teknologi MARA, 26400, Jengka, Pahang, Malaysia
**Institute of Science (IOS), Universiti Teknologi MARA, 40450, Shah Alam, Selangor, Malaysia
***Faculty of Applied Sciences, Universiti Teknologi MARA, 40450, Shah Alam, Selangor, Malaysia
†Corresponding author: Megat Ahmad Kamal Megat Hanafiah; makmh@uitm.edu.my

Nat. Env. & Poll. Tech.
Website: www.neptjournal.com

Received: 15-12-2019
Revised: 23-1-2020
Accepted: 28-03-2020

Key Words:
Adsorption
Coconut frond
EDTA dianhydride
Lead removal

ABSTRACT

Ethylenediaminetetraacetic dianhydride modified coconut frond (ECFP) was prepared, characterized and applied as a potential adsorbent to remove Pb(II) ions from aqueous solutions. Factors influencing adsorption such as pH of the solution, adsorbent dosage, Pb(II) concentration, contact time, and temperature were investigated. The optimum conditions for adsorption of Pb(II) ions were at pH 4 and dosage of 0.02 g. Adsorption reached its equilibrium state in 30 min for all Pb(II) concentrations. Chemisorption was suggested as the rate-limiting step as the adsorption process correlated well with the pseudo-second-order kinetics model. Based on adsorption isotherm results, Langmuir model fitted the experimental data well, and the maximum adsorption capacity was 84.03 $mg.g^{-1}$ at 300 K. Based on the thermodynamic study, Pb(II) adsorption occurred spontaneously with the enthalpy and entropy changes recorded were 0.0615 kJ mol^{-1} and 241.28 J K^{-1} mol^{-1}, respectively. It was found that the nature of adsorption was endothermic as the ΔH^{o} value obtained was positive.

INTRODUCTION

The release of non-bioessential heavy metals in the aquatic system has resulted in a serious environmental pollution issue. Lead (Pb) is listed as one of the harmful pollutants by World Health Organization due to its high propensity for biological accumulation, non-biodegradability and very toxic even presents at a low concentration (Bai et al. 2019, Cao et al. 2019). At Pb(II) ions concentration above 0.05 $mg.L^{-1}$ in drinking water, one might experience acute lead poisoning symptoms such as anaemia, hepatitis, nephritic syndrome, and encephalopathy. Excess exposure to Pb(II) ions might damage central nervous and gastrointestinal systems, liver and kidneys. For this reason, the United State Environmental Protection Agency (USEPA) had set the maximum standard concentration of Pb(II) ions in drinking water of 300 $\mu g.L^{-1}$ (Hu & Qiu 2019). Due to these reasons, various methods such as ion exchange, chemical precipitation, membrane filtration, and adsorption have been used to remove Pb(II) ions from wastewater (Cao et al. 2019).

In Malaysia, coconut (*Cocos nucifera*) is the third most important industrial crop after oil palm and rubber. In 2001, about 151 000 ha of land in Malaysia were used for coconut plantation and the value reduced gradually due to competition with oil palm plantation. As a result, the coconut industry revitalizing plan was carried out for replanting coconut trees between 2008 and 2015. This consequently raised another environmental issue, which was related to the disposal of coconut waste, as large quantities of coconut fronds were produced during pruning and silvicultural practices (Njoku et al. 2014, Shafie et al. 2012).

Ethylenediaminetetraacetic dianhydride (EDTAD) is a revivification of ethylenediaminetetraacetic acid (EDTA) with two additional anhydride groups on each molecule of EDTA. EDTAD is a biodegradable and powerful complexing agent due to the presence of carboxylic and amine groups (Júnior et al. 2009, Yu et al. 2008, Zhang et al. 2011). Several researchers had used EDTAD in modifying low-cost biomaterials such as neem leaf powder (Hanafiah et al. 2013), *Aloe vera* rind powder (Hanafiah et al. 2018), sugarcane bagasse (Júnior et al. 2009) and baker's yeast biomass (Xia et al. 2015, Yu et al. 2008, Zhang et al. 2011) to improve their adsorption performance. In this study, the adsorption behaviour of Pb(II) ions onto EDTAD modified coconut frond which included the effects of pH, dosage, concentration, contact time, and temperature were evaluated.

MATERIALS AND METHODS

Materials: Coconut fronds were collected from a coconut tree plantation located in Kelantan, Malaysia. The fronds were washed thoroughly, cut into small pieces, dried and washed with tap water to remove insoluble impurities before with deionized water. The fronds were dried in an oven at 333 K overnight before being ground and sieved by using a mechanical grinder to obtain the average particle size of 125-250 µm. The dried coconut frond powder was boiled in deionized water for 30 min to destroy microbes, washed and dried again in an oven overnight at 333 K. Ethylenediaminetetraacetic dianhydride (EDTAD) treatment was performed according to the method proposed by Hanafiah et al. (2013). Five grams of dried untreated coconut frond powder (UCFP) was added into the mixture of 0.50 g of EDTAD and 400 mL N, N-dimethylacetamide (DMAc) in a three-neck round bottom flask equipped with a condenser. The mixture was refluxed at 343 K for 24 h. The mixture was filtered and rinsed with 0.10 M NaOH thoroughly. The wet coconut frond powder was further rinsed with DMAc before finally rinsed with 4 L deionized water until the constant pH was obtained. The EDTAD treated coconut frond powder was dried in an oven at 333 K overnight and designated as ECFP.

Characterizations of ECFP: UCFP and ECFP were characterized by using an Attenuated Total Reflectance-Fourier Transform Infrared (ATR-FTIR) spectrometer (PerkinElmer, Spectrum 100, USA). Determination of pH_{zpc} of ECFP was done according to the method reported by Hanafiah et al. (2018) with some modification. A volume of 50 mL (0.01 M) KNO_3 was placed into different 100 mL conical flasks. The initial pH of this solution (pH_o) was adjusted from 2 to 10 by adding drops of 0.10 M HCl or NaOH solutions. A weight of 0.10 g ECFP was added into each flask and shaken in a water bath shaker for 24 h at 120 stroke min^{-1} at 300 K. ECFP was filtered and the final pH of KNO_3 solutions (pH_f) was measured using a pH meter.

Batch adsorption experiments: The analytical grade of 1000 $mg.L^{-1}$ stock solution of Pb(II) was obtained from Merck (Germany). Working concentration solutions of Pb(II) ions were prepared by appropriate dilutions. All adsorption experiments were done using 50 mL of 10 $mg.L^{-1}$ Pb(II) solutions (otherwise stated) and 0.02 g ECFP at 300 K and the shaking rate was 120 stroke min^{-1}. The effect of pH on adsorption of Pb(II) ions onto ECFP was done by adjusting the initial pH from 1 to 5 by adding drops of 0.10 M HCl and NaOH solutions. The effect of ECFP dosage on adsorption of Pb(II) ions was performed by varying the weight of ECFP (0.02 to 0.10 g) in Pb(II) ions solutions at pH 4. The mixtures were shaken for 90 min. In the kinetic study, the concentration of Pb(II) ions solutions was varied from 10 to 30 $mg.L^{-1}$ and the solutions were shaken at different time intervals (1, 3, 6, 10, 20, 30, 60, 90 and 120 min). The pH and the ECFP dosage were fixed at 4 and 0.02 g, respectively. Similar pH and adsorbent dosage were used in isotherm study, but the concentrations of Pb(II) ions were varied (5, 10, 15, 20, 25, 30, 40 and 75 $mg.L^{-1}$). The mixtures were then shaken for 90 min at 300 K. In the thermodynamic study, 5, 10, 15, 20, 25, 30, 40 and 75 $mg.L^{-1}$ Pb(II) ions solutions were shaken with 0.02 g ECFP for 90 min at different temperatures (303, 313 and 323 K). All experiments were done in duplicate. The mixtures were then filtered, and the final concentrations were analysed using an Atomic Absorption Spectrometer (AAS, PerkinElmer PinAAcle 900T, USA). The amount of adsorbed Pb(II) ions, q_e ($mg.g^{-1}$) and the removal percentage (%) of Pb(II) ions were calculated using eqs. (1) and (2), respectively.

$$q_e = \frac{C_i - C_f}{m} \times V \quad \ldots(1)$$

$$\text{Removal (\%)} = \frac{C_i - C_f}{C_i} \times 100 \quad \ldots(2)$$

Where, C_i and C_f are initial and final concentrations of Pb(II) ions ($mg.L^{-1}$), respectively, m is the weight of ECFP (g) and V is the volume of Pb(II) ions solutions (L).

RESULTS AND DISCUSSION

Characterizations of ECFP: Fig. 1 showed the FTIR spectra of UCFP, ECFP and Pb(II) loaded ECFP. A strong and broad band was observed at 3323 cm^{-1} in the FTIR spectra of UCFP. This might be attributed to the presence of O-H groups from cellulose, hemicellulose and lignin. Other peaks were observed at 1727, 1607, 1368, 1033, 898, and 562 cm^{-1} suggesting the presence of C=O, -NH, C-O, C-H, and =C-H. The presence of a new peak at 1736 cm^{-1} in ECFP could be attributed to the introduction of ester groups, as suggested by Pereira et al. (2010). Thus, it might suggest that EDTAD was successfully introduced onto UCFP by forming an ester with -OH groups from coconut frond (Júnior et al. 2009). After the adsorption of Pb(II) ions, the intensity of the peaks at 3323 and 1033 cm^{-1} was reduced, suggesting that -OH and C-O-C groups took part in the binding of Pb(II) ions during the adsorption process. Besides, there was a shift of peak at 1603 to 1593 cm^{-1} suggesting that a bond might be formed between Pb(II) ions and -NH groups.

The pH of zero point charge or pH_{zpc} was measured to determine the pH where the adsorbent had a zero net surface charge. Basically, at $pH=pH_{zpc}$, there were balance charges on the adsorbent surface. In general, at $pH < pHzpc$, an adsorbent surface tended to carry positive charges, while at $pH > pH_{zpc,}$ the adsorbent surface was negatively charged.

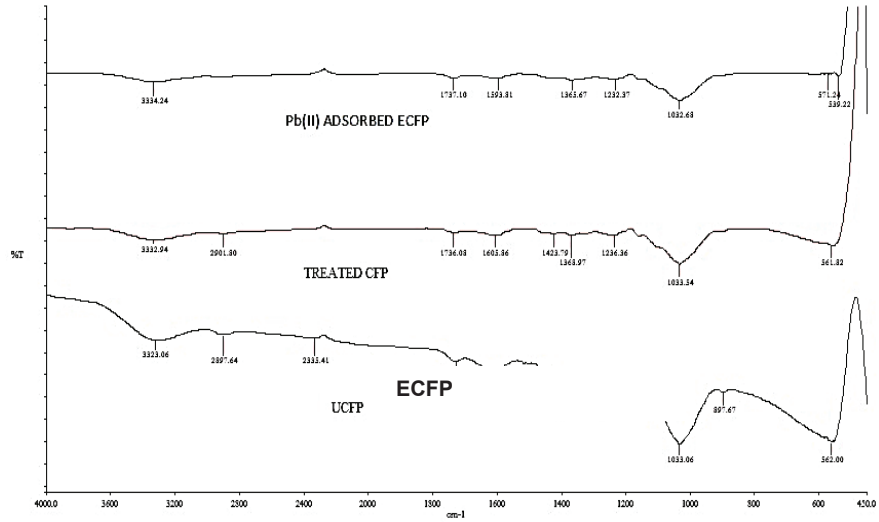

Fig. 1: FTIR spectra of UCFP, ECFP and Pb(II) ions adsorbed onto ECFP.

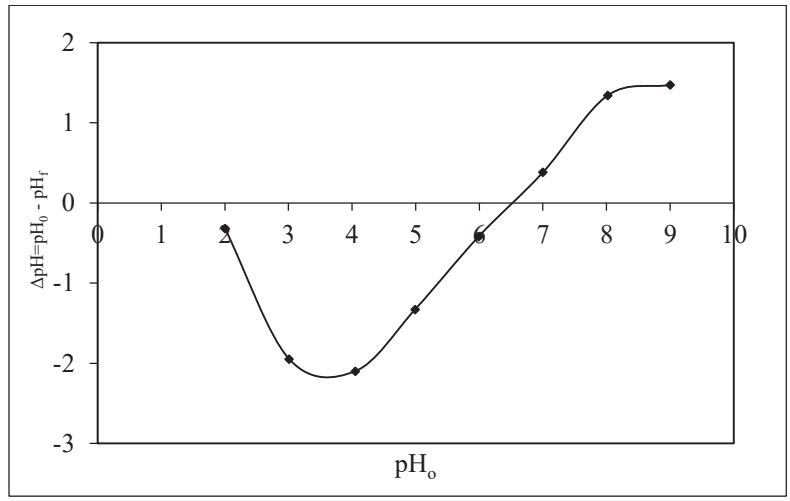

Fig. 2: pH_{zpc} plot of ECFP.

Therefore, the adsorption of a cationic metal is favoured when the pH was higher than pH_{zpc} (Srivastava et al. 2015). Fig. 2 shows the plot of pH_{zpc} of ECFP. The pH_{zpc} of ECFP was found at 6.4, based on the intersection point of the pH_o-axis. This indicated that when the pH of the solution was higher than 6.4, Pb(II) ions could have easily been attracted to the ECFP surface as more negative charges surrounded the adsorbent surface.

Effect of pH on adsorption of Pb(II) ions onto ECFP: The pH of a solution is a critical parameter in the adsorption of metal ions onto an adsorbent. The variation of pH might influence the affinity between adsorbent and adsorbate. To study the effect of initial pH on adsorption of Pb(II) ions onto ECFP, the initial pH of Pb(II) solution was varied from 1 to 5. Fig. 3 showed that low adsorption capacity, q_e was recorded at pH 1 (4.43 $mg.g^{-1}$). This could be explained by electrostatic repulsion of positively charged Pb(II) ions with positively charged adsorbent due to protonation of functional groups on the adsorbent surface or excessive cations from sorbed H^+ ions on the adsorbent surface itself (Ali et al. 2011, Faghihian et al. 2005, Torres-Blancas et al. 2013, Zhang et al. 2016)

The q_e value increased gradually with the increasing of initial pH of Pb(II) ions, where 7.25, 14.48, 22.20 and 23.45 mg.g-1 were recorded at pH 2, 3, 4 and 5, respectively. Basically, the increase of pH could lead to the reduction of repulsive force of the adsorbent surface towards the adsorbate

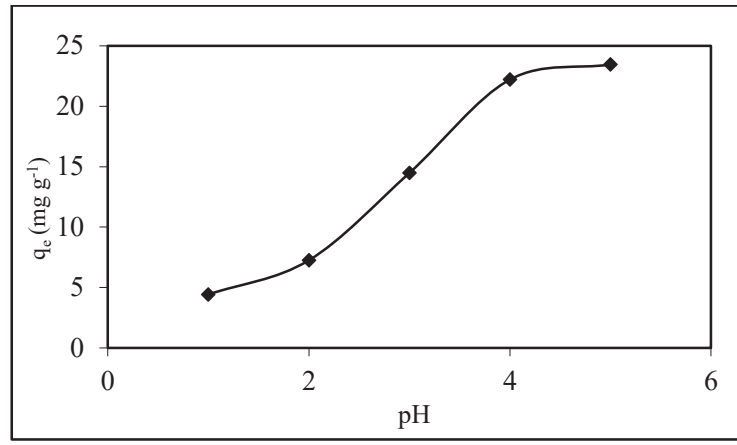

Fig. 3: Effect of pH on adsorption of Pb(II) ions onto ECFP (adsorbent weight: 0.02 g; volume: 50 mL; shaking rate: 120 stroke min^{-1}; equilibrium time: 90 min; Pb(II) concentration: 10 $mg.L^{-1}$).

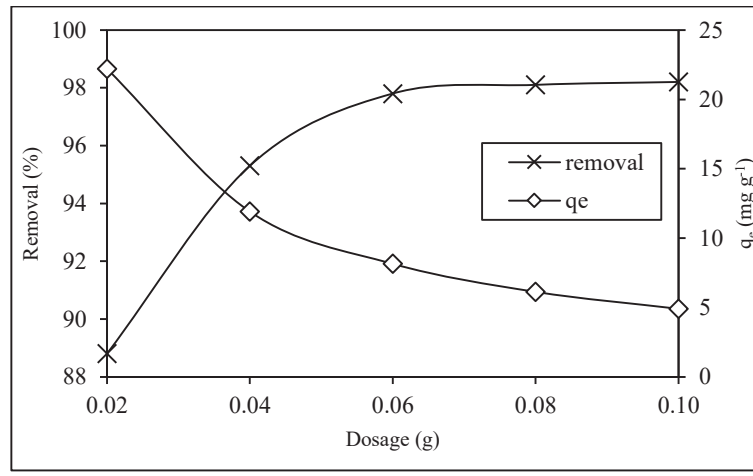

Fig. 4: Effect of adsorbent dosage on Pb(II) adsorption by ECFP (volume: 50 mL; pH: 4; shaking rate: 120 stroke min^{-1}; equilibrium time: 90 min; Pb(II) concentration: 10 $mg.L^{-1}$).

ion (Ali et al. 2011, Bhatnagar & Sillanpää 2009, Galhoum et al. 2015, Gok 2014) and thus promoted more adsorption sites as for the adsorption of metal ions. Furthermore, the number of protons (H^+) decreased with the increase of pH and thus reduced the competition between metal ions and H^+ for the adsorption sites (Miraoui et al. 2015, Torab-Mostaedi et al. 2015).

Effect of adsorbent dosage on adsorption of Pb(II) ions onto ECFP: The dosage of adsorbent was an important parameter as it strongly influenced the capacity of biosorption at a given initial concentration (Asgari et al. 2012). The dependence of adsorption of Pb(II) ions on the dosage of ECFP was shown in Fig. 4. The per cent of Pb(II) removal increased from 88.80 to 98.20 % for the adsorbent dosage of 0.02 g to 0.08 g, respectively. This could be attributed to the increase of surface area due to the increase of adsorbent weight or higher number of adsorption sites for a fixed concentration of Pb(II) (Mu et al. 2013). But, beyond dosage 0.08 g, there was no appreciable change in the percentage removal of Pb(II) because the number of Pb(II) ions became the limiting factor. The amount of Pb(II) ions adsorbed on the other hand showed the opposite trend. As more ECFP increased, the amount of Pb(II) ions adsorbed reduced. This was mainly due to the higher number of unsaturated adsorption sites when the dosage was increased, as stated in eq. (1).

Adsorption rate and kinetic models: Fig. 5 showed the effect of different concentrations on the adsorption rate of Pb(II) ions onto ECFP. Generally, the plots showed that the adsorption of Pb(II) ions involved two phases; the rapid adsorption pattern, and the slower, gradual adsorption rate

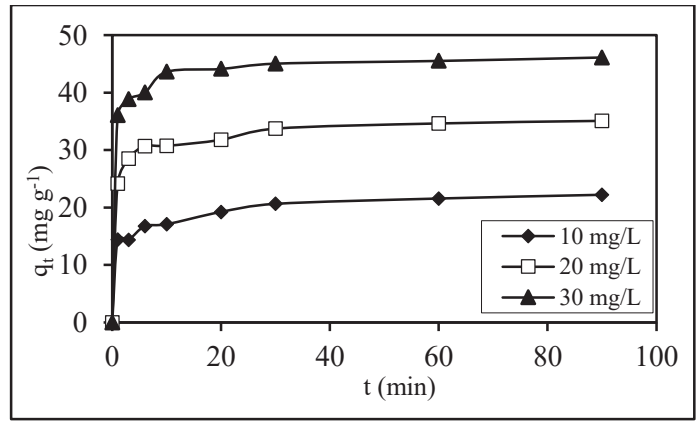

Fig. 5: Effect of contact time on different concentrations of Pb(II) ions for the adsorption of Pb(II) ions by ECFP (volume: 50 mL; pH: 4; shaking rate: 120 stroke min^{-1}; adsorbent dosage: 0.02 g).

until equilibrium uptake was achieved. At the beginning of the adsorption stage, a high amount of metal ions was adsorbed due to the high number of available active sites on the surface of the biosorbent. The actives sites were quickly occupied by the Pb(II) ions that led to a small difference in the change of adsorption rate after 10 min. Based on Fig. 5, it can be concluded that the amount of Pb(II) ions adsorbed increased proportionally with the initial concentration of Pb(II) ions. The amount of 10, 20 and 30 $mg.L^{-1}$ Pb(II) ions adsorbed were 22.20, 35.10 and 46.15 $mg.g^{-1}$, respectively. This situation could be explained by the increase in the driving force of the concentration gradient. The increase of driving force had overcome all the mass transfer resistance of metal ions from the aqueous phase to the solid phase, and subsequently provided a higher collision probability between metal ions and the active sites (Zhu et al. 2015). Overall, adsorption of Pb(II) ions onto ECFP showed relatively rapid adsorption process as equilibrium was achieved in less than 30 min for all Pb(II) concentrations. When the concentration of Pb(II) ions was low, the ratio of Pb(II) ions to the number of available adsorption sites was also low. Therefore, the adsorption sites seemed to take up the available Pb(II) ions much quickly since there was less competition among adsorbates ions (Gupta & Bhattacharyya 2008).

The rate of the adsorption of the metal ions is the momentum of the molecules to move from the aqueous solution to the adsorbent surface. In general, the adsorption process is governed by one or more mechanisms. Basically, adsorption process consists four stages (Srivastava et al. 2015), i.e; (i) the transfer of the solute from the solution to the boundary layer that surrounds the adsorbent surface, (ii) the transportation of the solute from the boundary layer to the adsorbent surface, (iii) the transfer of solute to the intraparticle sites from the adsorbent surface and (iv) the binding of solute ions to the available sites in the internal surface of the adsorbent.

Kinetics is the utmost important information for the adsorption study. A full-scale batch adsorption process can be obtained from the kinetics study. In addition, by applying certain adsorption kinetics models to the experimental data, one would gain a better understanding of the adsorption mechanism and the potential rate-limiting step (Sadeek et al. 2015, Zhang et al. 2016). Moreover, the rate of adsorption obtained through the kinetic study may help in optimizing the reactor dimension and residence time in any particular adsorption system (Sadeek et al. 2015). In this study, the pseudo-first (Ho & McKay 1998) and pseudo-second (Ho & McKay 2000) order kinetic models were used to determine the adsorption for the adsorption of Pb(II) ions onto ECFP and the linearized equations are given as follows:

$$\log(q_e - q_t) = \log q_{e,cal} - \frac{k_1}{2.303} t \qquad \ldots(3)$$

$$\frac{t}{q_t} = \frac{1}{k_2 q_{e,cal}^2} + \frac{1}{q_{e,cal}} t \qquad \ldots(4)$$

Where, t is time (min), $q_{e,cal}$ is the calculated adsorption capacity at equilibrium ($mg.g^{-1}$), q_t is the concentration of the analyte at time t ($mg.g^{-1}$), k_1 is pseudo-first-order rate constant (min^{-1}) and k_2 is pseudo-second-order rate constant (g mg^{-1} min^{-1}). Figs. 6 and 7 showed the plots of pseudo-first-order and pseudo-second-order kinetic models for the adsorption of 10, 20 and 30 $mg.L^{-1}$ Pb(II) ions onto ECFP at 300 K, respectively. The results analysed from both kinetics models are presented in Table 1.

In general, both pseudo-first and pseudo-second-order plots showed relatively good linearity ($R^2 > 0.85$), yet the pseudo-second-order kinetics model had a better agreement with the experimental data. This could be noticed from the values of R^2 that were almost unity (0.9990 to 0.9999) for

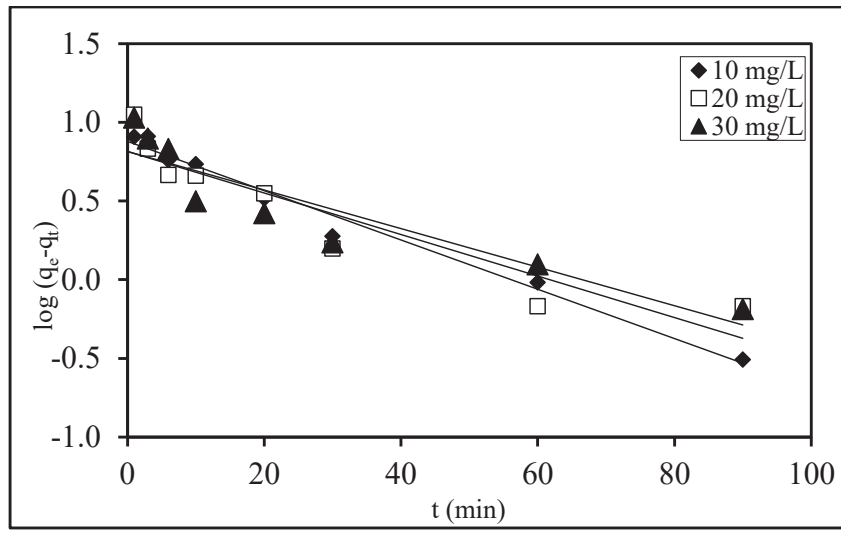

Fig. 6: Pseudo-first-order plots for the adsorption of Pb(II) ions onto ECFP (volume: 50 mL; pH: 4; shaking rate: 120 stroke min^{-1}; adsorbent dosage: 0.02 g; temperature: 300 K).

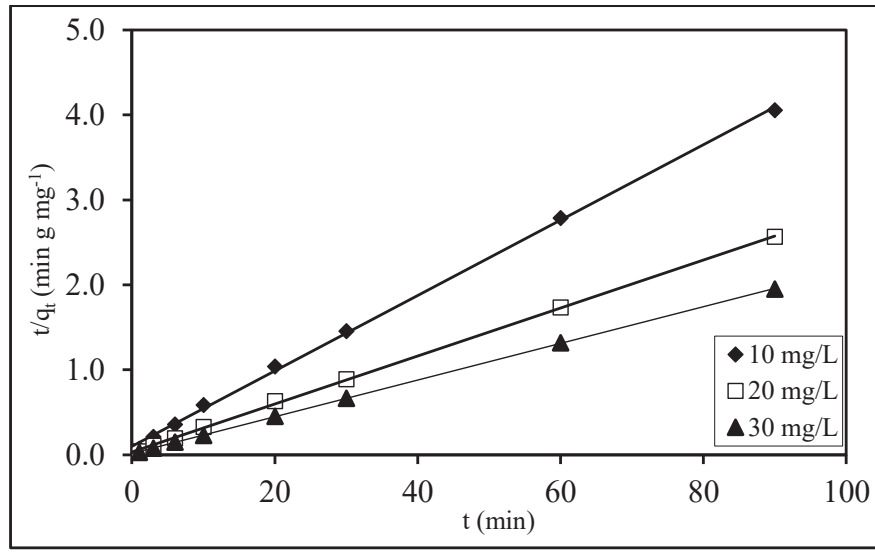

Fig. 7: Pseudo-second-order plots for the adsorption of Pb(II) ions onto ECFP (volume: 50 mL; pH: 4; shaking rate: 120 stroke min^{-1}; adsorbent dosage: 0.02 g; temperature: 300 K).

Table 1: Pseudo-first and pseudo-second-order parameters for adsorption of Pb(II) ions onto ECFP.

[Pb(II)] ($mg.L^{-1}$)	$q_{e,exp}$ ($mg.g^{-1}$)	Pseudo-first-order			Pseudo-second-order			
		k_1 ($mg.min^{-1}\ g^{-1}$)	$q_{e,cal}$ ($mg.g^{-1}$)	R^2	h ($mg.g^{-1}\ min^{-1}$)	k_2 ($mg.min^{-1}\ g^{-1}$)	$q_{e,cal}$ ($mg.g^{-1}$)	R^2
10	22.24	3.62×10^{-2}	7.56	0.982	10.06	1.98×10^{-2}	22.52	0.999
20	35.12	3.04×10^{-2}	6.53	0.862	30.12	2.41×10^{-2}	35.33	0.999
30	46.84	2.83×10^{-2}	6.54	0.850	64.94	3.03×10^{-2}	46.30	0.999

all concentrations, and the qe,cal values were very close to those recorded from the batch adsorption study. Due to this reason, chemisorption might govern the adsorption process, where metal ions bonded to the adsorbent through valance force, either by covalent bond through sharing of electrons or ion exchange mechanism (Galhoum et al. 2015, Gok 2014, Pasquier & Largitte 2016, Toor & Jin 2012, Wang et al. 2013).

Equilibrium and isotherm study: The equilibrium or adsorption isotherm describes the interaction of adsorbate with the adsorbent. It represents the distribution of different initial concentrations of solute at a constant temperature in the aqueous phase and solid phase. As adsorption isotherm provides that information, it turns as the most vital study in optimizing the adsorbent-adsorbate system, mechanistic pathways and understanding the adsorbent surface properties (Galhoum et al. 2015, Rangabhashiyam et al. 2014, Zhang et al. 2016).

To study the adsorption isotherm for the adsorption of Pb(II) ions onto ECFP, the initial concentration of Pb(II) ions was varied from 5 to 75 mg.L^{-1}. The mixtures were shaken for 90 min to ensure the equilibrium state. At the low concentrations of Pb(II) ions (<30 mg.L^{-1}), the sharp slope could be observed as presented in Fig. 8, an indication of a high-efficiency adsorbent for the adsorption of low metal ion concentrations. As the concentration of Pb(II) ions increased to 40 mg.L^{-1}, the slope reduced drastically. This condition was associated with the saturation of adsorption sites due to the increase in the ratio of the number of Pb(II) ions to the number of adsorption sites.

In general, the application of suitable isotherm models onto the experimental data is important as it can provide valuable information about the distribution of adsorption sites on the adsorbent surface, adsorption characteristic and affinity of adsorbent-adsorbate in the adsorption system. Several mathematical models can be applied to the experimental data such as two-parameter isotherm models which include Langmuir (Langmuir 1916) and Freundlich (Freundlich 1906). The linearized equations for Langmuir and Freundlich models are given in eqs. (5) and (6), respectively.

$$\frac{C_e}{q_e} = \frac{1}{bQ_{max,cal}} + \frac{C_e}{Q_{max,cal}} \quad \ldots(5)$$

$$\log q_e = \frac{1}{n}\log C_e + \log K_F \quad \ldots(6)$$

Where, q_e is the equilibrium adsorption capacity (mg.g^{-1}), $Q_{max,cal}$ is the maximum adsorption capacity (mg.g^{-1}), C_e is the equilibrium concentration of the adsorbate (mg.L^{-1}), b is the equilibrium constant (L mg^{-1}), K_F is a Freundlich constant (mg.g^{-1}) and n is a constant related to the heterogeneity of the adsorbent surface and its affinity for the adsorbate.

Figs. 9 and 10 showed Langmuir and Freundlich plots for adsorption of Pb(II) ions onto ECFP and the parameters for the isotherm models were listed in Table 2. In general, both isotherm models recorded high R^2 values (>0.92). Based on the agreement of experimental and theoretical values of Q_{max}, Langmuir isotherm model seemed to have a better fitting to the experimental data compared to Freundlich isotherm model. This condition might explain the monolayer coverage of Pb(II) ions on the ECFP surface.

Adsorption thermodynamics: To study the effect of different temperature on adsorption of Pb(II) ions, solutions ranged from 0 to 75 mg.L^{-1} was stirred with ECFP at 303, 313 and 323 K for 90 min. Fig. 11 showed the isotherm plot for the adsorption of Pb(II) ions at 303, 313 and 323 K. In general, adsorption of Pb(II) onto ECFP was more favourable

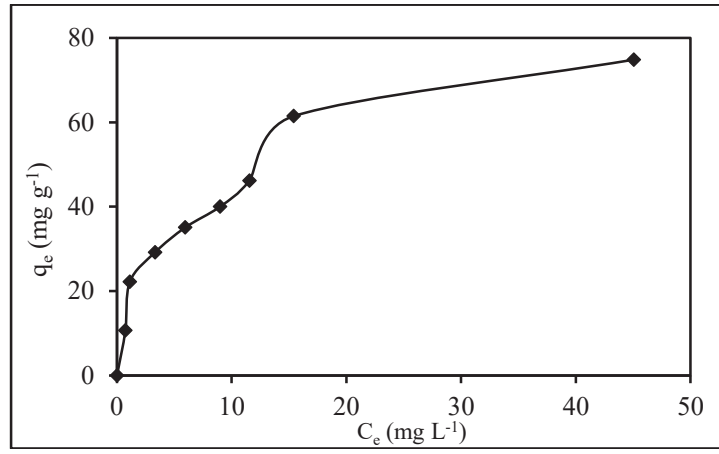

Fig. 8: Adsorption isotherm plot for adsorption of Pb(II) ions onto ECFP (volume: 50 mL; pH: 4; shaking rate: 120 stroke min^{-1}; adsorbent dosage: 0.02 g; temperature: 300 K).

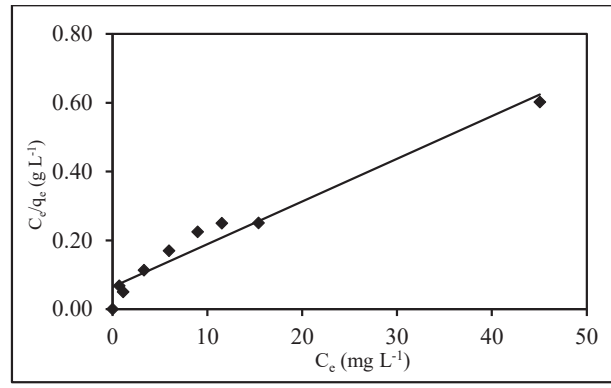

Fig. 9: Langmuir plot for adsorption of Pb(II) ions onto ECFP (volume: 50 mL; pH: 4; shaking rate: 120 stroke min^{-1}; adsorbent dosage: 0.02 g; temperature: 300 K).

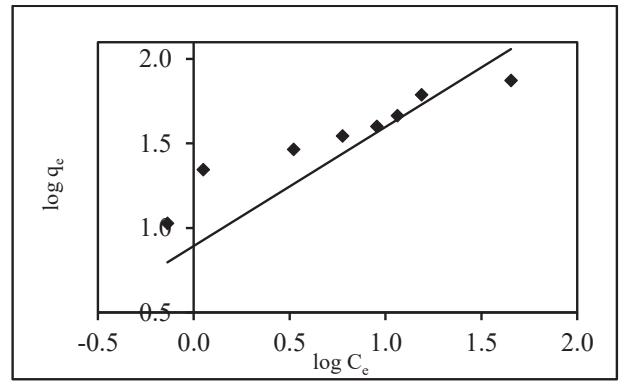

Fig. 10: Freundlich plot for adsorption of Pb(II) ions onto ECFP (volume: 50 mL; pH: 4; shaking rate: 120 stroke min^{-1}; adsorbent dosage: 0.02 g; temperature: 300 K).

Table 2: Langmuir and Freundlich isotherm parameters for adsorption of Pb(II) ions onto ECFP.

Temperature (K)	$q_{e,exp}$ (mg.g^{-1})	Langmuir			Freundlich		
		q_{max} (mg.g^{-1})	b (L.mg^{-1})	R^2	K_f	n	R^2
303	74.85	84.03	0.15	0.974	16.29	2.31	0.927

at higher temperatures as the recorded adsorption capacities increased with increasing temperatures, which also suggested an endothermic adsorption behaviour.

The thermodynamic parameters such as enthalpy ($\Delta H°$), entropy ($\Delta S°$), and Gibb's free energy ($\Delta G°$) were calculated to determine the adsorption process by using the following equations:

$$K_c = \frac{C_{ad}}{C_e} \quad \ldots(7)$$

$$\ln K_c = \frac{-\Delta H^o}{RT} + \frac{\Delta S^o}{R} \quad \ldots(8)$$

$$\Delta G^o = -RT \ln K_c \quad \ldots(9)$$

Where, K_c is the equilibrium constant, C_{ad} is the concentration of Pb(II) ions adsorbed on solid at equilibrium (mmol.L^{-1}), C_e is the equilibrium concentration of Pb(II) ions in the solution (mmol.L^{-1}), R is the gas constant (8.314 J K^{-1} mol^{-1}) and T is the temperature in Kelvin. Fig. 12 showed the Van't Hoff plot for the adsorption of Pb(II) ions onto ECFP at 303, 313 and 323 K. The calculated values for $\Delta H°$, $\Delta S°$, and $\Delta G°$ were listed in Table 3. In general, all $\Delta G°$ values for the adsorption of Pb(II) at 303, 313 and 323 K were negative, an indication of spontaneous adsorption process at those temperatures. The positive $\Delta H°$ value recorded in this study indicated that adsorption of Pb(II) ions onto ECFP was endothermic, where adsorption was more favourable at a higher temperature. Meanwhile, the positive $\Delta S°$ value suggested that this process was an entropy-driven process where a higher degree of freedom of the ions was obtained at a higher temperature.

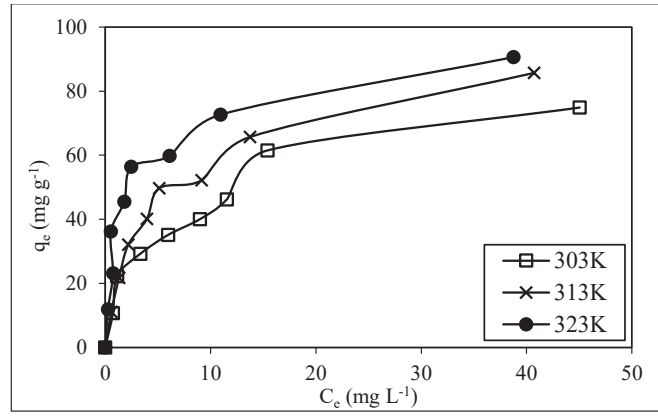

Fig. 11: Adsorption isotherm plots of Pb(II) ions onto ECFP at 303, 313 and 323 K (volume: 50 mL; pH: 4; shaking rate: 120 stroke min^{-1}; adsorbent dosage: 0.02 g).

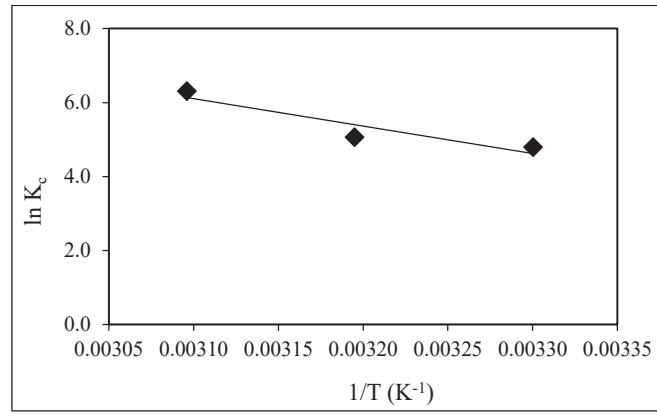

Fig. 12: Van't Hoff plot for adsorption of Pb(II) ions onto ECFP (adsorbent weight: 0.02 g; volume: 50 mL; pH: 4; shaking rate: 120 stroke min^{-1}, Pb concentration: 5-75 mg.L^{-1}; equilibrium time 90 min).

Table 3: Thermodynamic parameters for adsorption of Pb(II) ions onto ECFP.

Temperature	ΔG^o (kJ mol^{-1})	ΔH^o (kJ mol^{-1})	ΔS^o (J mol^{-1})
303	-13.14	0.0615	241.28
313	-13.16		
323	-16.95		

CONCLUSION

The current work revealed the potential application of ECFP as an adsorbent for removing Pb(II) ions from aqueous solutions. The amount of Pb(II) ions adsorbed was reduced in a highly acidic condition and the optimum adsorption pH range was 4 to 5. The satisfactory adsorption capacity was recorded from the Langmuir isotherm model with the q_{max} value of 84.03 mg.g^{-1} being recorded. The potential functional groups responsible for adsorbing Pb(II) ions as revealed by the FTIR spectra were hydroxyl, amino, carbonyl, aromatics and ether. Adsorption process could be considered rapid due to the short time taken to reach equilibrium stage for all concentrations of Pb(II) ions. Based on the thermodynamic study, Pb(II) ions were more favoured to be adsorbed at a higher temperature, suggesting an endothermic adsorption behaviour.

REFERENCES

Ali, O.I.M., Osman, H.H., Sayed, S.A. and Shalabi, M.E.H. 2011. The removal of some rare earth elements from their aqueous solutions on by-pass cement dust (BCD). Journal of Hazardous Materials, 195: 62-67.

Asgari, G., Roshani, B. and Ghanizadeh, G. 2012. The investigation of kinetic and isotherm of fluoride adsorption onto functionalize pumice stone. Journal of Hazardous Materials, 217-218: 123-132.

Bai, J., Chao, Y., Chen, Y., Wang, S. and Qiu, R. 2019. The effect of interaction between *Bacillus subtilis* DBM and soil minerals on Cu(II) and Pb(II) adsorption. Journal of Environmental Sciences (China), 78: 328-337.

Bhatnagar, A. and Sillanpää, M. 2009. Applications of chitin- and chitosan-derivatives for the detoxification of water and wastewater-A short review. Advances in Colloid and Interface Science, 152(1-2): 26-38.

Cao, Y., Xiao, W., Shen, G., Ji, G., Zhang, Y., Gao, C. and Han, L. 2019. Carbonization and ball milling on the enhancement of Pb(II) adsorption by wheat straw: Competitive effects of ion exchange and precipitation. Bioresource Technology, 273: 70-76.

Faghihian, H., Amini, M.K. and Nezamzadeh, A.R. 2005. Cerium uptake by zeolite A synthesized from natural clinoptilolite tuffs. Journal of Radioanalytical and Nuclear Chemistry, 264(3): 577-582.

Freundlich, H. 1906. Über die adsorption in läosungen. Journal of Physical Chemistry, 57: 385-470.

Galhoum, A.A., Mahfouz, M.G., Abdel-Rehem, S.T., Gomaa, N.A., Atia, A.A., Vincent, T. and Guibal, E. 2015. Diethylenetriamine-functionalized chitosan magnetic nano-based particles for the sorption of rare earth metal ions [Nd(III), Dy(III) and Yb(III)]. Cellulose, 22(4): 2589-2605.

Gok, C. 2014. Neodymium and samarium recovery by magnetic nano-hydroxyapatite. Journal of Radioanalytical and Nuclear Chemistry, 301: 641-651.

Gupta, S.S.G. and Bhattacharyya, K. 2008. Immobilization of Pb(II), Cd(II) and Ni(II) ions on kaolinite and montmorillonite surfaces from aqueous medium. Journal of Environmental Management, 87: 46-58.

Hanafiah, M.A.K.M., Jamaludin, S.Z.M., Khalid, K. and Ibrahim, S. 2018. Methylene blue adsorption on aloe vera rind powder: Kinetics, isotherm and mechanisms. Nature Environment and Pollution Technology, 17: 1055-1064.

Hanafiah, M.A.K.M., Ismail, M., Ngah, W.S.W., Wan Mat Khalir, W.K.A. and Zakaria, H. 2013. Adsorption behavior of methylene blue on ethylenediaminetetraacetic dianhydride modified neem (*Azadirachta indica)* leaf powder. Key Engineering Materials, 594-595(December): 270-274.

Ho, Y.S. and McKay, G. 1998. A comparison of chemisorption kinetic models applied to pollutant removal on various sorbents. Process Safety and Environmental Protection, 76(4): 332-340.

Ho, Y.S. and McKay, G. 2000. The kinetics of sorption of divalent metal ions onto sphagnum moss peat. Water Research, 34: 735-742.

Hu, C. and Qiu, M. 2019. Characterization of the biochar derived from peanut shell and adsorption of Pb(II) from aqueous solutions. Nature Environment and Pollution Technology, 18: 225-230.

Júnior, O.K., Gurgel, L.V A., de Freitas, R.P. and Gil, L.F. 2009. Adsorption of Cu(II), Cd(II), and Pb(II) from aqueous single metal solutions by mercerized cellulose and mercerized sugarcane bagasse chemically modified with EDTA dianhydride (EDTAD). Carbohydrate Polymers, 77(3): 643-650.

Langmuir, I. 1916. The constitution and fundamental properties of solids and liquids. Journal of American Chemical Society, 38: 2221-2295.

Miraoui, A., Didi, M.A. and Villemin, D. 2015. Neodymium(III) removal by functionalized magnetic nanoparticles. Journal of Radioanalytical and Nuclear Chemistry, 307: 963-971.

Mu, N., ALOthman, Z. A. and Khan, M. R. 2013. Removal of malathion from aqueous solution using De-Acidite FF-IP resin and determination by UPLC–MS/MS: Equilibrium, kinetics and thermodynamics studies. Talanta, 115: 15-23.

Njoku, V.O., Islam, M.A., Asif, M. and Hameed, B.H. 2014. Preparation of mesoporous activated carbon from coconut frond for the adsorption of carbofuran insecticide. Journal of Analytical and Applied Pyrolysis, 110(1): 172-180.

Pasquier, R. and Largitte, L. 2016. A review of the kinetics adsorption models and their application to the adsorption of lead by an activated carbon. Chemical Engineering Research and Design, 109: 495-504.

Pereira, F.V., Gurgel, L.V.A. and Gil, L.F. 2010. Removal of Zn^{2+} from aqueous single metal solutions and electroplating wastewater with wood sawdust and sugarcane bagasse modified with EDTA dianhydride (EDTAD). Journal of Hazardous Materials, 176: 856-863.

Rangabhashiyam, S., Anu, N., Giri Nandagopal, M.S. and Selvaraju, N. 2014. Relevance of isotherm models in biosorption of pollutants by agricultural byproducts. Journal of Environmental Chemical Engineering, 2(1), 398-414.

Sadeek, S.A., Negm, N.A., Hefni, H.H.H. and Wahab, M.M.A. 2015. Metal adsorption by agricultural biosorbents: Adsorption isotherm, kinetic and biosorbents chemical structures. International Journal of Biological Macromolecules, 81: 400-409.

Shafie, S.M., Mahlia, T.M.I., Masjuki, H.H. and Ahmad-Yazid, A. 2012. A review on electricity generation based on biomass residue in Malaysia. Renewable and Sustainable Energy Reviews, 16(8): 5879-5889.

Srivastava, S., Agrawal, S.B. and Mondal, M.K. 2015. Biosorption isotherms and kinetics on removal of Cr(VI) using native and chemically modified *Lagerstroemia speciosa* bark. Ecological Engineering, 85: 56-66.

Toor, M. and Jin, B. 2012. Adsorption characteristics, isotherm, kinetics, and diffusion of modified natural bentonite for removing diazo dye. Chemical Engineering Journal, 187: 79-88.

Torab-Mostaedi, M., Asadollahzadeh, M., Hemmati, A. and Khosravi, A. 2015. Biosorption of lanthanum and cerium from aqueous solutions by grapefruit peel: equilibrium, kinetic and thermodynamic studies. Research on Chemical Intermediates, 41: 559-573.

Torres-Blancas, T., Roa-Morales, G., Fall, C., Barrera-Díaz, C., Ureña-Nuñez, F. and Pavón Silva, T. B. 2013. Improving lead sorption through chemical modification of de-oiled allspice husk by xanthate. Fuel, 110: 4-11.

Wang, F., Zhao, J., Wei, X., Huo, F., Li, W., Hu, Q. and Liu, H. 2014. Adsorption of rare earths (III) by calcium alginate-poly glutamic acid hybrid gels. Journal of Chemical Technology and Biotechnology, 89(7): 969-977.

Wang, Y., Wang, X., Wang, X., Liu, M., Wu, Z., Yang, L., Xia, S. and Zhao, J. 2013. Adsorption of Pb(II) from aqueous solution to Ni-doped bamboo charcoal. Journal of Industrial Engineering Chemistry, 19: 353-359.

Xia, Y., Yao, Q., Zhang, W., Zhang, Y. and Zhao, M. 2015. Comparative adsorption of methylene blue by magnetic baker's yeast and EDTAD-modified magnetic baker's yeast: Equilibrium and kinetic study. Arabian Journal of Chemistry, 12(8): 2448-2456.

Yu, J., Tong, M., Sun, X. and Li, B. 2008. Enhanced and selective adsorption of Pb^{2+} and Cu^{2+} by EDTAD-modified biomass of baker's yeast. Bioresource Technology, 99(7): 2588-2593.

Zhang, L., Zeng, Y. and Cheng, Z. 2016. Removal of heavy metal ions using chitosan and modified chitosan : A review. Journal of Molecular Liquids, 21: 175-191.

Zhang, Y., Zhu, J., Zhang, L., Zhang, Z., Xu, M. and Zhao, M. 2011. Synthesis of EDTAD-modified magnetic baker's yeast biomass for Pb^{2+} and Cd^{2+} adsorption. Desalination, 278(1-3): 42-49.

Zhu, H.X., Cao, X.J., He, Y.C., Kong, Q.P., He, H. and Wang, J. 2015. Removal of Cu^{2+} from aqueous solutions by the novel modified bagasse pulp cellulose: Kinetics, isotherm and mechanism. Carbohydrate Polymers, 129: 115-126.